# BRANCHED TWO-MANIFOLDS SUPPORTING ALL LINKS [1]

ROBERT W. GHRIST[2]
*Center for Applied Mathematics*
*Cornell University*
*Ithaca, NY, 14853*

**Abstract**

We resolve several conjectures of J. Birman and R. F. Williams concerning the knotting and linking of closed orbits of flows on 3-manifolds. Our methods center on the symbolic dynamics of semiflows on branched 2-manifolds, or templates. By proving the existence of "universal templates," or embedded branched 2-manifolds supporting all finite links, we conclude that the set of closed orbits of any flow transverse to the fibration of the figure-eight knot complement in $S^3$ contains representatives of every (tame) knot and link isotopy class.

In these notes, we will answer some questions raised by Birman and Williams in their original examination of the link of closed orbits in the flow on $S^3$ induced by the fibration of the complement of a knot or link [5] (see §4 for definitions). In this work, they proposed the following conjecture:

**Conjecture 1 (Birman and Williams, 1983)** *The figure-eight knot does not appear as a closed orbit of the flow induced by the fibration of the complement of the figure-eight knot in $S^3$.*

By "the" fibration, we mean the unique fibration whose monodromy is the pseudo-Anosov representative of its isotopy class, with respect to the Thurston classification [34, 9]. By "the" flow, we mean the flow obtained by integrating the gradient of the fibration: it is everywhere normal to the fibres.

We resolve this conjecture, and in so doing, unearth some surprising facts about flows on 3-manifolds (via semiflows on branched 2-manifolds). Our main results, announced in [16], are as follows:

**Theorem 3** There exists an embedded branched 2-manifold in $S^3$ with semiflow whose closed orbits contain representatives of every link isotopy class.

**Theorem 4** Any flow transverse to a fibration over $S^1$ of the figure-eight knot complement in $S^3$ contains representatives of every link isotopy class as closed orbits.

To assist us, we adopt certain perspectives from symbolic dynamics for labeling and manipulating infinite sublinks of an infinite link. We will include only those definitions and methods which are relevant to the context of this paper, leaving a more detailed exposition of the symbolic methods and the dynamical implications to a more comprehensive work [15].

---

[1] To appear in *Topology*.

[2] Current address: Program in Applied & Computational Mathematics, Princeton University; Princeton, NJ, 08544-1000. rwghrist@math.princeton.edu

# 1 BACKGROUND

Periodic orbits of a flow are embedded circles. When the flow is three-dimensional, periodic orbits are knots and the collection of periodic orbits forms a link which often is nontrivial. Since there is an underlying flow structure for these objects, the link comes to us oriented. We follow the (not-so-standard) convention of [4, 5, 23, 20, 22, 33, 13] for signed crossings displayed in Figure 1.

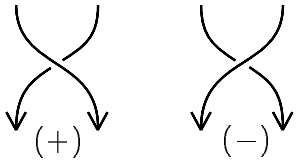


**FIGURE 1: Positive and negative crossings**

The principal tool for examining knotted periodic orbits in three dimensional flows is the template construction of Birman and Williams [4, 5].

**Definition 1** *A* TEMPLATE *(also known as a knotholder) is a compact branched two-manifold with boundary and with smooth expanding semiflow, built from local* BRANCH LINE CHARTS*, displayed in Figure 2(a).*

For an equivalent definition, with examples, see [4, 5]. The term *semi*flow denotes an action of $\mathbb{R}^+$ as opposed to $\mathbb{R}$ and is necessary since the flow is not uniquely reversible at the branch lines. By *expansive* we mean that the return map on the branch lines induced by the semiflow is an expanding map: i.e., any sufficiently small subinterval is stretched to a larger one. Each branch line in the template will locally appear as in Figure 2(a): there will be a certain number ($\geq 2$) of incoming strips which completely cover the branch line (expanding the incoming semiflow), and a certain number ($\geq 2$) of outgoing strips. The incoming and outgoing strips of all the branch lines are then connected bijectively. In Figure 2(b), we show the simplest example of a template: the Lorenz template [4, 36, 37], consisting of one branch line and two strips.

A template thus consists of a finite set of branch lines connected by strips. Though this description differs slightly from the "joining and splitting chart" description in [4, 5], it is nevertheless equivalent and serves to facilitate a symbolic approach to templates (as will be explained).

Strictly speaking, the template itself is not invariant under the semiflow as some orbits may "escape" through gaps in the branch lines. However, since no closed orbits can exit through a gap, we may ignore the escaping orbits.

The relationship between templates and links of periodic orbits in three dimensional flows is expressed in the Template Theorem:

**Theorem 1 (Birman and Williams, 1983)** *Given a flow on a three-manifold having a hyperbolic chain-recurrent set (i.e., Axiom A plus no-cycle), the link of periodic orbits*

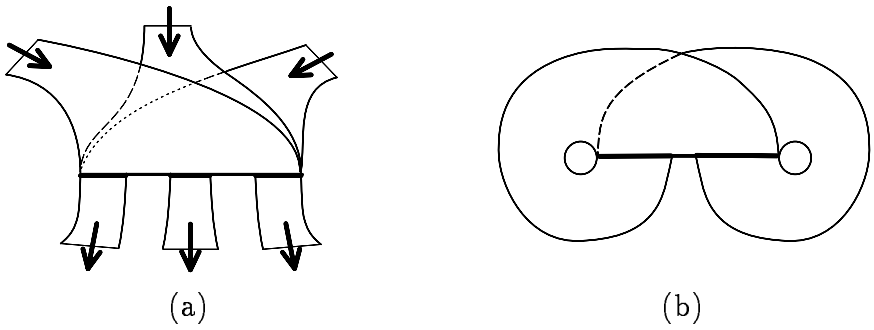


**FIGURE 2: (a) strips meet at a branch line (b) the Lorenz template**

*is in bijective correspondence with the link of periodic orbits on a particular embedded template (with at most two exceptions). On any finite sublink, this correspondence is via ambient isotopy.*

We refer the reader to [6, 29, 18, 27] for definitions concerning hyperbolicity and chain-recurrence, which are not necessary for the remainder of this paper. Intuitively, this hyperbolicity condition requires the existence of uniform expanding and contracting directions along the flow. The template is derived by collapsing out the contracting direction (a strong stable foliation) of the original flow, changing the flow on a three-manifold to a semiflow on a branched two-manifold. In cases where the entire flow is hyperbolic, one must first "split" the flow along at most two orbits, thus giving rise to fictitious additional periodic orbits (the occasional "exceptions" of Theorem 1) — see [5, 15] for the precise construction, the details of which are not vital to the present work. Theorem 1 acts as a method of dimension reduction for the problem of understanding the periodic orbits of the original flow, and greatly facilitates the analysis of knotting and linking. Aside from their relevance to the dynamics of flows, we argue in this work that templates are in their own right a fascinating class of objects.

Let $\mathcal{T}$ denote a template embedded in $S^3$. The study of $\mathcal{T}$ has traditionally taken one of two forms. Often, one studies the topological properties of the individual closed orbits on $\mathcal{T}$. For example, one might prove a result on the types of torus knots that $\mathcal{T}$ supports [23, 4] or what bounds on the genus or the prime decomposition of individual closed orbits exist [4, 5, 31, 33]. This perspective has been of greatest use in concocting invariants for bifurcations of periodic orbits in flows [23, 19, 20, 21, 13]. The following conjecture, concerning the "spectrum" of individual knots that any template may support, was also posed in [5]:

**Conjecture 2 (Birman and Williams, 1983)** *There does not exist an embedded template which supports all (tame) knots as periodic orbits of the semiflow: i.e., a* UNIVERSAL TEMPLATE.

The other principal perspective is to examine the topological properties of $\mathcal{T}$ in its own right — this is often surprisingly subtle. A fundamental problem in the study of

templates is the equivalence problem: **when are two templates equivalent?** We must, however, carefully specify what we mean by equivalence. Though the matter has not been clearly treated in the literature, the "implied" definition one finds is the following:

**Definition 2** *Two embedded templates are equivalent if their periodic orbit sets can be placed in a bijective correspondence which preserves isotopy classes of every finite sublink.*

For the remainder of this paper, we will adopt this as the definition for template equivalence, though our results imply that it is neither the most useful nor the most natural definition. Under Definition 2, one may cut a template along *nonperiodic* orbits of the semiflow and isotope the resulting object without changing the template equivalence class. There are other "moves" on templates which preserve template equivalence classes (see [5] for examples), but it is important to note that the moves which generate template equivalence (the analogue of the Reidemeister moves in knot theory) are not completely known. Even if there were a finite set of moves, there is no reason to believe that equivalent templates can be realized through a finite sequence of such moves, since the underlying links are infinite.

In this work, we adopt and develop a different perspective (first considered in [20, 31]) which, instead of considering either the entire template or the individual orbits, focuses on something of intermediate size.

**Definition 3** *A* SUBTEMPLATE $\mathcal{S}$ *of a template* $\mathcal{T}$ *is a subset of* $\mathcal{T}$ *which, under the restriction of the semiflow of* $\mathcal{T}$ *to* $\mathcal{S}$*, satisfies Definition 1.*

Subtemplates can be thought of as "connected" proper infinite sublinks. Examples will appear later in Figures 4, 5, and 6. Subtemplates are obtained through removing portions of $\mathcal{T}$ by cutting along periodic and nonperiodic orbits of the semiflow. M. Sullivan has discovered some surprising behavior in the subtemplate structure of templates having a combination of positive and negative crossings (template crossings having the same convention as crossings in Figure 1) [33]. His insights were the starting points for the present work, which came about while reformulating his results using symbolic methods.

In §2, we establish our conventions for the symbolic description of knots on templates and introduce methods for identifying subtemplates through simple maps on spaces of symbol sequences. In §3, we apply these techniques to resolve Conjecture 2. We then turn to the study of fibred knots and links in §4 and answer Conjecture 1.

This work is intended to complement the existing literature on template theory. The seminal works in this field are the two papers of Birman and Williams [4, 5] (foreshadowed by Williams [36, 37]). The series of papers by Holmes and Williams [23] and Holmes [20, 21] lay the foundation for applying templates to bifurcations in a family of Hénon maps (see [13, 15] for surveys). Franks [10] along with Williams [37, 38] have used templates to contribute to the relationship between dynamics and knot types [11]. Polynomial invariants for template knots are considered in [12]. More recent work on topological properties has been conducted by M. Sullivan [30, 33, 31]. Finally, the paper of Mindlin *et al.* [26] has initiated the use of templates in time series data analysis (see also [35, 24]). This is by no means a complete survey of references for this growing field.

# 2 SYMBOLIC DYNAMICS AND INFLATIONS

The utility of symbolic dynamics for describing orbits in hyperbolic sets of dynamical systems (*e.g.*, the Smale horseshoe map) is well known [6, 27]. The same is true in describing knots on templates [36, 37, 5, 13]. Consider a template $\mathcal{T}$ composed of strips, each of which connects two (not necessarily distinct) branch lines. Assign to the strips the labels $x_1, x_2, \ldots, x_N$: this forms a Markov partition for the return map induced by the semiflow on the branch lines. Hence, every forward orbit (periodic or nonperiodic) may be assigned a unique semi-infinite symbol sequence in the $x_i$ symbols given by the order in which it traverses the various strips. This symbol sequence is the orbit's ITINERARY [36, 37, 25]. The ITINERARY SET for a template $\mathcal{T}$ is denoted

$$\Sigma_{\mathcal{T}} = \{\mathbf{a} = a_0 a_1 a_2 \ldots : \mathbf{a} \text{ is an itinerary of an orbit on } \mathcal{T}\} \quad (1)$$

$$\subset \{x_1, x_2, \ldots, x_N\}^{\mathbf{Z}^+} . \quad (2)$$

The itinerary set $\Sigma_{\mathcal{T}}$ does not consist of all possible strings of symbols, but only those strings which are ADMISSIBLE [6, 27]. We will refer to the elements of the Markov partition $\{x_1, x_2, \ldots, x_N\}$ as the GENERATORS of $\Sigma_{\mathcal{T}}$. In the case of a periodic orbit, the itinerary is also periodic and may be referred to by the corresponding finite word of minimal period: *e.g.*, $x_1x_2x_1x_2\ldots = (x_1x_2)^\infty$.

The way in which orbits fit together on a template is described by placing a "coordinate system" on each branch line and then pushing these coordinates forward to the itinerary space $\Sigma_{\mathcal{T}}$. The kneading theory [36, 37, 25] establishes this coordinate system for the symbol sequences in $\Sigma_{\mathcal{T}}$ through an ordering, $\lhd$, which reflects the ordering of the points on the branch line from which the orbits commence.

For a given template $\mathcal{T}$, one simply specifies an appropriate ordering among all generators of the itinerary set whose corresponding orbits commence from the same branch line. For orientable templates, itineraries may then be ordered "lexicographically" with respect to $\lhd$. Ordering itineraries on nonorientable templates is no more difficult, but it does require more bookkeeping. We now illustrate these concepts via a set of examples which are central to the remaining work.

**Example 1** Let $\mathcal{U}_n$ and $\mathcal{V}_n$ ($n \in \mathbf{Z}$) be the families of embedded templates pictured in Figure 3, outfitted with the Markov partitions $\{x_1, \ldots, x_4\}$ as labeled. The subscript $n$ refers to the number of (signed) full twists in the $x_4$ strip: in other words, there are $2n$ half-twists (positive or negative as per the sign) in the $x_4$ strip. Examples of these templates were first studied by M. Sullivan with the notation $A$ (our $\mathcal{V}_0$) and $B$ (our $\mathcal{U}_0$) [33].

The kneading ordering for these templates[3] is:

$$\mathcal{U}_n : \begin{array}{l} x_1 \lhd x_2 \\ x_4 \lhd x_3 \end{array} \qquad \mathcal{V}_n : \begin{array}{l} x_1 \lhd x_2 \\ x_3 \lhd x_4 \end{array} . \quad (3)$$

[3]The apparent reversal of ordering on the second branch line of $\mathcal{V}_n$ is imposed to preserve a symmetry, to be exploited in Proposition 2.

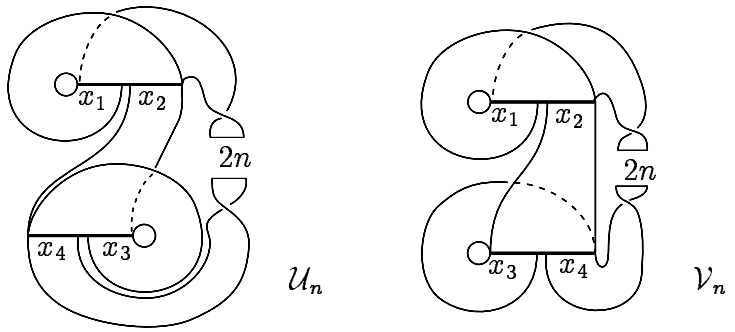


**FIGURE 3: The templates $\mathcal{U}_n$ and $\mathcal{V}_n$ — the subscript refers to the $2n$ signed half-twists in the $x_4$ strip.**

Since these templates each have two branch lines, there are two $\lhd$-orderings: one for each branch line. For example, on the upper branch line of $\mathcal{V}_n$, $x_1^2 x_2 x_3 \ldots \lhd x_1 x_2 x_3 \ldots \lhd x_2 x_3 \ldots$

For a given template $\mathcal{T}$ endowed with a Markov partition $x_1, \ldots, x_N$, every branch line of $\mathcal{T}$ may be further decomposed into BRANCH SEGMENTS via the Markov partition. A branch segment, $\beta_i(\mathcal{T})$ for $i = 1..N$, can be thought of as the closed interval of the branch line from which the $x_i$-strip emanates; symbolically,

$$\beta_i(\mathcal{T}) = \{\mathbf{a} \in \Sigma_{\mathcal{T}} : a_0 = x_i\}. \tag{4}$$

The left and right endpoints (with respect to $\lhd$) of each $\beta_i(\mathcal{T})$ will be denoted $\partial_i^\ell(\mathcal{T})$ and $\partial_i^r(\mathcal{T})$ respectively. These orbits are eventually periodic and each forms a portion of the boundary of $\mathcal{T}$.

**Example 2** Each of the templates $\mathcal{U}_n$ ($\mathcal{V}_n$) has two branch lines, and these each contain two branch segments from whence the strips emanate. Hence, the symbolic BRANCH SET $\beta(\mathcal{U}_n)$ ($\beta(\mathcal{V}_n)$) consists of a total of four "closed intervals": $\beta_i(\mathcal{U}_n)$ ($\beta_i(\mathcal{V}_n)$) for $i = 1..4$, corresponding to the four elements of the Markov partition.

$$\beta(\mathcal{U}) = \{\beta_1(\mathcal{U}) \cup \beta_2(\mathcal{U})\},\ \{\beta_3(\mathcal{U}) \cup \beta_4(\mathcal{U})\} \tag{5}$$

$$\begin{aligned}
\beta_1(\mathcal{U}) = [\partial_1^\ell(\mathcal{U}), \partial_1^r(\mathcal{U})] &= [(x_1)^\infty, x_1 x_2 (x_3)^\infty] \\
\beta_2(\mathcal{U}) = [\partial_2^\ell(\mathcal{U}), \partial_2^r(\mathcal{U})] &= [x_2 x_4 (x_1)^\infty, x_2 (x_3)^\infty] \\
\beta_3(\mathcal{U}) = [\partial_3^\ell(\mathcal{U}), \partial_3^r(\mathcal{U})] &= [x_3 x_4 (x_1)^\infty, (x_3)^\infty] \\
\beta_4(\mathcal{U}) = [\partial_4^\ell(\mathcal{U}), \partial_4^r(\mathcal{U})] &= [x_4 (x_1)^\infty, x_4 x_2 (x_3)^\infty]
\end{aligned}$$

$$\beta(\mathcal{V}) = \{\beta_1(\mathcal{V}) \cup \beta_2(\mathcal{V})\},\ \{\beta_3(\mathcal{V}) \cup \beta_4(\mathcal{V})\} \tag{6}$$

$$\begin{aligned}
\beta_1(\mathcal{V}) = [\partial_1^\ell(\mathcal{V}), \partial_1^r(\mathcal{V})] &= [(x_1)^\infty, x_1 (x_2 x_4)^\infty] \\
\beta_2(\mathcal{V}) = [\partial_2^\ell(\mathcal{V}), \partial_2^r(\mathcal{V})] &= [x_2 (x_3)^\infty, (x_2 x_4)^\infty] \\
\beta_3(\mathcal{V}) = [\partial_3^\ell(\mathcal{V}), \partial_3^r(\mathcal{V})] &= [(x_3)^\infty, x_3 (x_4 x_2)^\infty] \\
\beta_4(\mathcal{V}) = [\partial_4^\ell(\mathcal{V}), \partial_4^r(\mathcal{V})] &= [x_4 (x_1)^\infty, (x_4 x_2)^\infty]
\end{aligned}$$

Since these symbolic descriptions are independent of the number of full twists in the $x_4$ branch, we have omitted the subscripts for $\mathcal{U}_n$ and $\mathcal{V}_n$.

Although the symbolic data for a given template neither encodes the topology of the template nor provides invariants for orbits, it does become useful in extracting certain subtemplate structures through a construction which we call a TEMPLATE INFLATION.

**Definition 4** *A* TEMPLATE INFLATION *of a template $\mathcal{S}$ into a template $\mathcal{T}$ is a map $\mathfrak{R} : \mathcal{S} \hookrightarrow \mathcal{T}$ taking orbits to orbits which is a diffeomorphism onto its image.*

**Remark 1** The image of a template inflation $\mathfrak{R} : \mathcal{S} \hookrightarrow \mathcal{T}$ is clearly a subtemplate.

The kernel of Definition 4 is that the image of the induced subtemplate $\mathfrak{R}(\mathcal{S})$ has the same *dynamics* as $\mathcal{S}$. This does not imply that $\mathfrak{R}(\mathcal{S})$ holds the same knots or has the same topological features as $\mathcal{S}$.

In the case where an inflation $\mathfrak{R}$ maps $\mathcal{T} \hookrightarrow \mathcal{T}$, we say that $\mathfrak{R}$ is a TEMPLATE RENORMALIZATION, since one can interpret $\mathfrak{R}$ as a renormalization of the induced return map of the semiflow on the branch segments [15]; however, it is more enlightening for our purposes to think in terms of subtemplates. The image $\mathfrak{R}(\mathcal{T}) \subset \mathcal{T}$ is a subtemplate of $\mathcal{T}$ which is diffeomorphic to $\mathcal{T}$.

For $\mathcal{S}$ and $\mathcal{T}$ embedded templates, a template inflation $\mathfrak{R} : \mathcal{S} \hookrightarrow \mathcal{T}$ induces a topological action on periodic orbits of $\mathcal{S}$. Inflations which preserve the isotopy class of the link of periodic orbits will be of particular importance in this paper (other types of inflations are useful; e.g., in the study of the suspended Smale horseshoe map [15, 13, 20]).

**Definition 5** *Let $\mathfrak{R} : \mathcal{S} \hookrightarrow \mathcal{T}$ be an inflation of a template $\mathcal{S} \subset S^3$ into a template $\mathcal{T} \subset S^3$. Let $i_{\mathcal{S}}$ and $i_{\mathcal{T}}$ denote inclusion of $\mathcal{S}$ and $\mathcal{T}$ respectively into $S^3$. If $i_{\mathcal{S}}$ and $i_{\mathcal{T}} \circ \mathfrak{R}$ are isotopic embeddings of $\mathcal{S}$ in $S^3$, then $\mathfrak{R}$ is an* ISOTOPIC INFLATION.

The image of an isotopic inflation is a subtemplate $\mathfrak{R}(\mathcal{S})$ isotopic to $\mathcal{S}$. Therefore, one says that $\mathcal{T}$ contains $\mathcal{S}$ as a subtemplate: $\mathcal{S} \subset \mathcal{T}$.

The key ingredients for our results are the combination of isotopic inflations, which allow us to keep track of the topology of orbits, and the related action on orbit itineraries, which allows for symbolic computation of "deeply" embedded orbits:

**Lemma 1** *A template inflation $\mathfrak{R} : \mathcal{S} \hookrightarrow \mathcal{T}$ induces a map $\mathfrak{R} : \Sigma_{\mathcal{S}} \hookrightarrow \Sigma_{\mathcal{T}}$ whose action is to inflate each generator $\{x_i : i = 1..N\}$ of $\Sigma_{\mathcal{S}}$ to a finite admissible word $\{w_i : i = 1..N\}$ in the generators of $\Sigma_{\mathcal{T}}$.*

*Proof:* By continuity, $\mathfrak{R}$ maps the branch lines of $\mathcal{S}$ into the branch lines of $\mathcal{T}$. Hence, each strip of $\mathcal{S}$ (corresponding to a generator $x_i$ of $\Sigma_{\mathcal{S}}$) is mapped to a finite sequence of strips in $\mathcal{T}$, corresponding to a finite admissible word. □

The image under $\mathfrak{R}$ of any orbit on $\mathcal{S}$ is thus obtained by "inflating" each symbol $x_i$ in the itinerary by the word $w_i$ (which in some cases may consist of $x_i$ alone). This immediately implies the following useful result:

**Corollary 1** *Given $\mathfrak{R} : \mathcal{S} \hookrightarrow \mathcal{T}$ a template inflation, the branch segments of the subtemplate $\mathfrak{R}(\mathcal{S})$ are given by*

$$\beta_i(\mathfrak{R}(\mathcal{S})) = \mathfrak{R}(\beta_i(\mathcal{S})) = \{\mathfrak{R}(\mathbf{a}); \mathbf{a} \in \beta_i(\mathcal{S})\}\,. \tag{7}$$

Returning to the families of templates in Example 1, we will use isotopic inflations to keep track of arbitrarily deep copies of $\mathcal{U}_n$ and $\mathcal{V}_n$ in each other. By starting with a few simple inflations that can be easily visualized, we can compose very complicated subtemplate structures. A special case $(m, n = 0)$ of the following theorem appears in [33]:

**Theorem 2** *For any $m, n \in \mathbb{Z}$, the following isotopic template inflations exist:*

$$\mathcal{U}_m \subset \mathcal{U}_n; \qquad \mathcal{V}_m \subset \mathcal{V}_n; \qquad \mathcal{U}_m \subset \mathcal{V}_n; \qquad \mathcal{V}_m \subset \mathcal{U}_n. \tag{8}$$

We first establish a few simple isotopic inflations with which we build the inflations of Theorem 2.

**Proposition 1** *The following are isotopic template inflations:*

$$\mathfrak{D}: \begin{array}{l} \mathcal{U}_{n+1} \hookrightarrow \mathcal{U}_n \\ \mathcal{V}_{n+1} \hookrightarrow \mathcal{V}_n \end{array} \qquad \begin{cases} x_1 \mapsto x_1 \\ x_2 \mapsto x_1 x_2 \\ x_3 \mapsto x_3 \\ x_4 \mapsto x_4 \end{cases}, \tag{9}$$

$$\mathfrak{F}: \mathcal{U}_{-1} \hookrightarrow \mathcal{V}_0 \qquad \begin{cases} x_1 \mapsto x_1 \\ x_2 \mapsto x_2 x_3 \\ x_3 \mapsto x_4 x_2 \\ x_4 \mapsto x_4 \end{cases}, \tag{10}$$

$$\mathfrak{G}: \mathcal{V}_0 \hookrightarrow \mathcal{U}_0 \qquad \begin{cases} x_1 \mapsto x_1 \\ x_2 \mapsto x_1 \\ x_3 \mapsto x_2 x_4 \\ x_4 \mapsto x_2 x_3 x_4 \end{cases}. \tag{11}$$

This is shown by drawing the image of the given inflation and noting that it is an isotopic copy of the domain. Figure 4 gives the proof for $\mathfrak{D}$ acting on $\mathcal{V}_0$: the other cases follow in like manner and are a simple exercise. Figures 5 and 6 give the proofs for $\mathfrak{F}$ and $\mathfrak{G}$ respectively.

The following two propositions specify the inherent symmetries among the various $\mathcal{U}_n$ and $\mathcal{V}_n$ which we will later exploit:

**Proposition 2** *For every $n \in \mathbb{Z}$, the inflation*

$$\chi: \begin{array}{l} \mathcal{U}_n \to \mathcal{U}_{-n} \\ \mathcal{V}_n \to \mathcal{V}_{-n} \end{array} \qquad \begin{cases} x_1 \mapsto x_3 \\ x_2 \mapsto x_4 \\ x_3 \mapsto x_1 \\ x_4 \mapsto x_2 \end{cases} \tag{12}$$

*takes any orbit to its mirror image: i.e., $\chi$ reverses all crossings.*

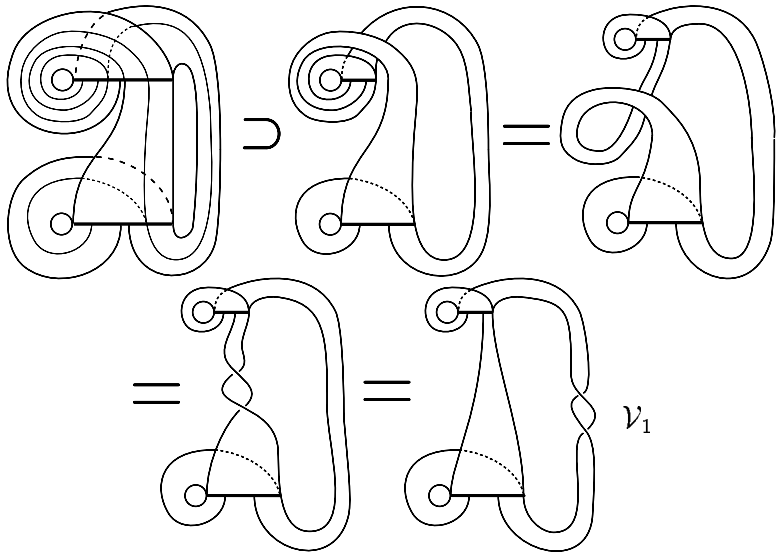


**FIGURE 4: The action of $\mathfrak{D}$ is via isotopy**

*Proof:* Consider first the case $n = 0$; then $\chi : \mathcal{U}_0 \to \mathcal{U}_0$ ($\mathcal{V}_0 \to \mathcal{V}_0$) is an involution which acts on the branch lines by exchanging them. Hence, $\chi$ reverses all crossings in this case. For $n \neq 0$, the additional crossings in the $x_4$-strip associated with $\mathcal{U}_n$ ($\mathcal{V}_n$) are reversed in specifying the range as $\mathcal{U}_{-n}$ ($\mathcal{V}_{-n}$). Since the action of $\chi$ is again to exchange the upper and lower branch lines, all of the crossings have been reversed. □

Consider the space of all isotopic inflations among the family of templates $\{\mathcal{U}_n, \mathcal{V}_n : n \in \mathbf{Z}\}$. The non-isotopic inflation $\chi$ induces an involution on this space via conjugation:

**Proposition 3** *Fix $m$ and $n$ arbitrary integers. Choose $\mathcal{Y}$ to represent either the symbol $\mathcal{U}$ or $\mathcal{V}$ (for example, if $\mathcal{Y} = \mathcal{U}$ then $\mathcal{Y}_0$ is the template $\mathcal{U}_0$). Choose $\mathcal{Z}$ to represent either $\mathcal{U}$ or $\mathcal{V}$ as well. Given any inflation $\mathfrak{R} : \mathcal{Y}_m \hookrightarrow \mathcal{Z}_n$ which acts isotopically, the*

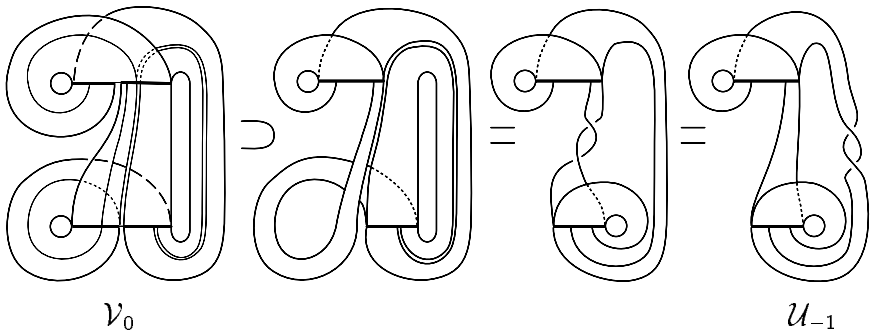


**FIGURE 5: The action of $\mathfrak{F}$ is via isotopy**

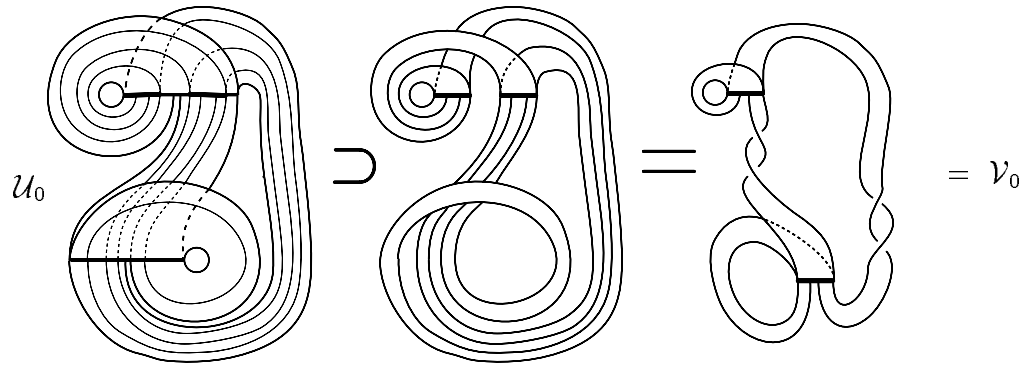


**FIGURE 6: The action of $\mathfrak{G}$ is via isotopy**

CONJUGATE INFLATION,

$$\begin{aligned} \mathfrak{R}^* \quad &: \quad \mathcal{Y}_{-m} \xrightarrow{\chi} \mathcal{Y}_m \overset{\mathfrak{R}}{\hookrightarrow} \mathcal{Z}_n \xrightarrow{\chi} \mathcal{Z}_{-n} && (13) \\ &= \quad \chi\mathfrak{R}\chi : \mathcal{Y}_{-m} \hookrightarrow \mathcal{Z}_{-n} && (14) \end{aligned}$$

*acts isotopically as well.*

*Proof:* The topological action of $\chi$ (reversing all crossings) commutes with the topological action of $\mathfrak{R}$ (isotopy), even though the symbolic actions do not commute. Hence, on the topological level, $\mathfrak{R}^*$ acts as $\chi^2\mathfrak{R}$. By Proposition 2, the topological action of $\chi^2$ is trivial; hence, $\mathfrak{R}^*$ acts via isotopy. □

Taking conjugates allows us to build new isotopic inflations: e.g.,

$$\mathfrak{F}^* : \mathcal{U}_1 \hookrightarrow \mathcal{V}_0 \qquad \begin{cases} x_1 \mapsto x_2 x_4 \\ x_2 \mapsto x_2 \\ x_3 \mapsto x_3 \\ x_4 \mapsto x_4 x_1 \end{cases} . \tag{15}$$

**Remark 2** For any inflations $\mathfrak{R}$ and $\tilde{\mathfrak{R}}$, $(\mathfrak{R}\tilde{\mathfrak{R}})^* = \mathfrak{R}^*\tilde{\mathfrak{R}}^*$ since $\chi$ is involutive.

*Proof of Theorem 2*: one may use the inflations $\mathfrak{D}$, $\mathfrak{F}$, and $\mathfrak{G}$ along with their conjugates in various combinations. For example, to find an isotopic copy of $\mathcal{U}_{-3}$ in $\mathcal{U}_0$, we may apply $(\mathfrak{D}^*)^3$ or $\mathfrak{G}\mathfrak{F}(\mathfrak{D}^*)^2$ to the orbits of $\mathcal{U}_{-3}$. Of course, many such inflations are available. □

The inflations $(\mathfrak{D}\mathfrak{D}^*)$, $\mathfrak{G}$, and $\mathfrak{G}^*$ appear pictorially in the work of M. Sullivan [33], without the symbolic description. The simple inflations $\mathfrak{D}$, $\mathfrak{F}$, and $\mathfrak{G}$, and their conjugates allow us to easily specify complicated subtemplates within this family of templates: e.g.,

**Proposition 4** *There exists a countable collection of isotopic copies of $\mathcal{V}_0$ embedded in $\mathcal{V}_0 \subset S^3$ as subtemplates which are disjoint and (completely) separable.*

*Proof:* Consider the inflations $\mathfrak{G}$ and $\mathfrak{G}^*$ which each map $\mathcal{V}_0 \to \mathcal{U}_0$ isotopically. We claim that the images of $\mathcal{V}_0$ under $\mathfrak{G}$ and $\mathfrak{G}^*$ are disjoint (except at a common boundary) and separable. Using Corollary 1, one computes the images of the branch set $\beta(\mathcal{V}_0)$ under $\mathfrak{G}$ and $\mathfrak{G}^*$ and uses the $\lhd$-ordering to prove that the branch lines, hence the subtemplates, are disjoint. In Figure 7, we display the two embedded subtemplates after crushing out the direction transverse to the semiflow (for ease of visualization), yielding two graphs, which can be seen to be separable. Alternatively, one can refer to Fig. 2.3 of [33].

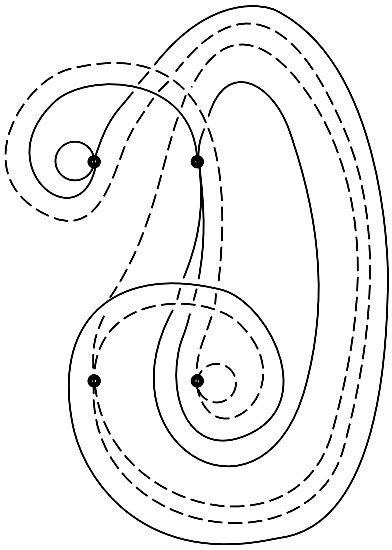

**FIGURE 7: The subtemplates $\mathfrak{G}(\mathcal{V}_0)$ and $\mathfrak{G}^*(\mathcal{V}_0)$, presented as graphs, are separable**

Consider the inflations $\mathfrak{FDG}$ and $\mathfrak{FDG}^*$ which take $\mathcal{V}_0 \hookrightarrow \mathcal{V}_0$ isotopically by Proposition 1. Since $\mathfrak{D}$ and $\mathfrak{F}$ act isotopically, the images of $\mathfrak{FDG}$ and $\mathfrak{FDG}^*$ are also disjoint and separable. Consider the sequence of template inflations

$$\{\mathcal{A}_n\}_{n=0}^{\infty} = \{(\mathfrak{FDG})\,(\mathfrak{FDG}^*)^n : \; n = 0..\infty\}\,. \tag{16}$$

Each $\mathcal{A}_n$ has as its image a subtemplate of $\mathcal{V}_0$ which is isotopic to $\mathcal{V}_0$. Since the images of $\mathfrak{FDG}$ and $\mathfrak{FDG}^*$ are disjoint and separable, it follows that the images of $\mathcal{A}_n = (\mathfrak{FDG})\,(\mathfrak{FDG}^*)^n$ and of $\mathcal{B}_n = (\mathfrak{FDG}^*)^{n+1}$ are likewise disjoint and separable. But the image of $\mathcal{B}_n$ contains the image of every $\mathcal{A}_k$ for $k > n$ as a subtemplate, since

$$\mathcal{A}_k = (\mathfrak{FDG})\,(\mathfrak{FDG}^*)^{k-n-1}\,(\mathfrak{FDG}^*)^{n+1} = (\mathfrak{FDG})\,(\mathfrak{FDG}^*)^{k-n-1}\,\mathcal{B}_n. \tag{17}$$

This implies that the subtemplates corresponding to the images of the inflations $\mathcal{A}_n$ are disjoint and separable, not only pairwise but also completely. □

When combined with Theorem 2, the above result holds for any $\mathcal{U}_n$ or $\mathcal{V}_n$: a surprising fact. Already, this seemingly simple family of templates displays a surprising richness.

In the next section, we will use the actions of "deep" isotopic inflations on the branch segments ($\beta$) and the boundaries ($\partial$) to keep track of where and how certain subtemplates

are situated, even though we can no longer visualize them. This will assist us in answering Conjecture 2.

# 3 UNIVERSAL TEMPLATES

Having developed the necessary template theory and examples, we state our main theorem:

**Theorem 3** *The embedded template $\mathcal{V}_0$ contains an isotopic copy of every (tamely embedded) knot and link as periodic orbits of the semiflow.*

*Proof:* Consider the templates $\mathcal{W}_q$, $q > 0$, pictured in Figure 8. These templates are embedded $q$-fold covers of $\mathcal{V}_0$, though we do not depend on this fact for the proof. Note in particular that the sign of the crossings in the sequence of "ears" along the bottom alternates. It should be clear that there is a natural sequence of subtemplate inclusions

$$\mathcal{V}_0 \equiv \mathcal{W}_1 \subset \mathcal{W}_2 \subset \cdots \subset \mathcal{W}_q \subset \cdots . \tag{18}$$

Our strategy is to show that the converse is also true: $\mathcal{W}_q$ is a subtemplate of $\mathcal{V}_0$ for every $q$. Then, we show that any closed braid appears as a set of closed orbits of every $\mathcal{W}_q$ for $q$ greater than some $Q < \infty$.

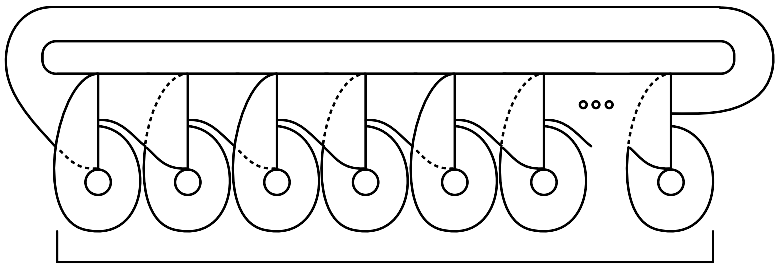


**FIGURE 8: The template $\mathcal{W}_q$**

The template $\mathcal{W}_1$ is isotopic to $\mathcal{V}_0$. We build $\mathcal{W}_q$ by "sewing in" positive and negative (with respect to our sign convention) ears to a deeper copy of $\mathcal{W}_{q-1}$ in $\mathcal{V}_0$. At each stage, we use a series of isotopic inflations to push the original copy of $\mathcal{V}_0$ deeper and deeper into itself, maneuvering the boundary components of the image of the original $\mathcal{V}_0$ for the next ear to be added. This manipulation of subtemplates is fairly difficult and requires some symbolic bookkeeping.

In order to apply an iterative argument, we need to exploit the symmetry in $\mathcal{V}_0$ expressed by $\chi$:

**Lemma 2** *$\chi$ is $\lhd$-preserving on $\mathcal{V}_n$: i.e., $\chi(\lhd) = \lhd$. Furthermore, $\chi$ has the following action on the branch segments and boundary components:*

$$\begin{array}{rcl} \chi : \mathcal{V}_n \to \mathcal{V}_{-n} & & \\ \beta_1(\mathcal{V}) & \leftrightarrow & \beta_3(\mathcal{V}) \\ & & \partial_1^\ell(\mathcal{V}) \leftrightarrow \partial_3^\ell(\mathcal{V}) \\ & & \partial_1^r(\mathcal{V}) \leftrightarrow \partial_3^r(\mathcal{V}) \\ \beta_2(\mathcal{V}) & \leftrightarrow & \beta_4(\mathcal{V}) \\ & & \partial_2^\ell(\mathcal{V}) \leftrightarrow \partial_4^\ell(\mathcal{V}) \\ & & \partial_2^r(\mathcal{V}) \leftrightarrow \partial_4^r(\mathcal{V}). \end{array} \tag{19}$$

*Proof:* That $\chi$ is $\lhd$-preserving follows from checking that Equation (3) is invariant under $\chi$. The action of $\chi$ on $\beta_i(\mathcal{V})$ is to take the first symbol, $x_i$, to $\chi(x_i)$; hence, $\chi(\beta_i(\mathcal{V})) = \beta_j(\mathcal{V})$ where $j$ equals the index of $\chi(x_i)$. The action of $\chi$ on $\partial_i^{\ell/r}(\mathcal{V})$ can be computed directly from Equation (6). $\square$

The following important lemma deals with a modification for subtemplates of $\mathcal{V}_n$ which we denote APPENDING AN EAR.

**Lemma 3** *Let $\mathcal{T}$ be a subtemplate of $\mathcal{V}_n$ which does not contain the orbit $(x_1)^\infty$. Define $I = [\partial^\ell(I), \partial^r(I)]$ to be the component of $\mathcal{T} \cap (\beta_1(\mathcal{V}) \cup \beta_2(\mathcal{V}))$ which is minimal with respect to $\lhd$ on the upper branch line of $\mathcal{V}_n$. Then, there exists a subtemplate $\mathcal{T}^+$ satisfying $\mathcal{T} \subset \mathcal{T}^+ \subset \mathcal{V}_n$ which is isotopic to the union of $\mathcal{T}$ and a positive ear appended along the new branch line $[(x_1)^\infty, \partial^r(I)]$. The subtemplate $\mathcal{T}^+$ contains the orbit $\partial_4^\ell(\mathcal{V})$.*

*Proof:* Since the subtemplate $\mathcal{T}$ avoids the $(x_1)^\infty$ component of the boundary of $\mathcal{V}_0$, the interval $I = [\partial^\ell(I), \partial^r(I)]$ cannot be part of $\beta(\mathcal{T})$, the branch set of $\mathcal{T}$; otherwise, one of the strips of $\mathcal{T}$ which terminates at the branch line must come from the $x_1$ strip, contradicting the minimality of $I$. Since $\mathcal{T}$ does not intersect $\beta(\mathcal{V})$ in the points between $(x_1)^\infty$ and $\partial^\ell(I)$, we may create here a new branch line by adding a new ear about the $x_1$ strip of $\mathcal{V}_n$ and "thickening" the incoming $x_4$ strip: see Figure 9.

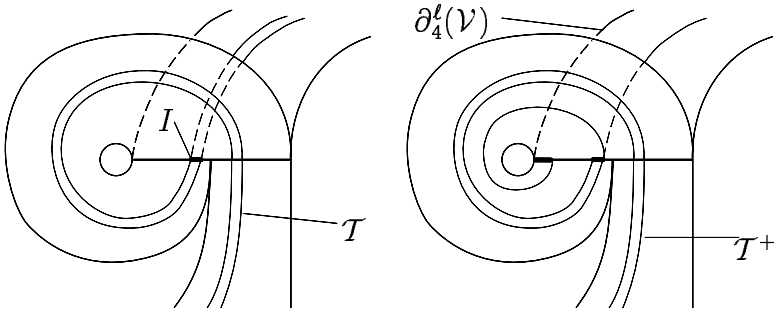


**FIGURE 9: Appending an ear to a subtemplate $\mathcal{T}$**

Specifically, for any $\partial^{\ell/r}(\mathcal{T})$ which contains the itinerary $\partial^{\ell}(I)$, we replace this block with $(x_1)^{\infty}$. Define two new branch segments for $\mathcal{T}^+$:

$$\begin{aligned} \beta_{N+1}(\mathcal{T}^+) &= [(x_1)^{\infty}, x_1\partial^r(I)] \\ \beta_{N+2}(\mathcal{T}^+) &= I = [\partial^{\ell}(I), \partial^r(I)]. \end{aligned} \tag{20}$$

This is the formal description of $\mathcal{T}^+$, which is a subtemplate in accordance with Definition 3: what we have really done is added a new ear along the $x_1$ strip which is of positive sign. We note that the new template $\mathcal{T}^+$ is isotopic to the original $\mathcal{T}$ in every way except for the addition of the ear and the thickened strip(s) — of course, appending an ear adds many new orbits to a subtemplate. Since the orbit $(x_1)^{\infty}$ is separable (it links no other orbit of $\mathcal{V}_0$), the appended ear does not link any other strip of $\mathcal{T}$. The subtemplate $\mathcal{T}^+$ contains $\partial_4^{\ell}(\mathcal{V})$ as part of its boundary, since $\partial_4^{\ell}(\mathcal{V})$ flows into $(x_1)^{\infty}$. □

We may exploit the symmetry of $\mathcal{V}_n$ expressed in Lemma 2 to obtain a conjugate result:

**Lemma 4** *Let $\mathcal{T}$ be a subtemplate of $\mathcal{V}_n$ which does not contain the orbit $(x_3)^{\infty}$. Define $I = [\partial^{\ell}(I), \partial^r(I)]$ to be the component of $\mathcal{T} \cap (\beta_3(\mathcal{V}) \cup \beta_4(\mathcal{V}))$ which is minimal with respect to $\lhd$ on the lower branch line of $\mathcal{V}_n$. Then, there exists a subtemplate $\mathcal{T}^-$ satisfying $\mathcal{T} \subset \mathcal{T}^- \subset \mathcal{V}_n$ which is isotopic to the union of $\mathcal{T}$ with a negative ear appended along the new branch line $[(x_3)^{\infty}, \partial^r(I)]$. The subtemplate $\mathcal{T}^-$ contains the orbit $\partial_2^{\ell}(\mathcal{V})$.*

*Proof:* Apply $\chi : \mathcal{V}_n \to \mathcal{V}_{-n}$ to send $\mathcal{T}$ to its mirror image $\mathcal{T}^* \subset \mathcal{V}_{-n}$ (as per Proposition 2). By applying Lemma 2, one checks that $\mathcal{T}^*$ and $\chi(I)$ satisfy the hypotheses of Lemma 3; hence, there exists a copy of $(\mathcal{T}^*)^+$ in $\mathcal{V}_{-n}$ which is isotopic to the mirror image of $\mathcal{T}$ with an added positive ear along the branch line $[(x_1)^{\infty}, \chi\partial^r(I)]$. Apply $\chi$ again to send $\mathcal{V}_{-n}$ back to $\mathcal{V}_n$ and $(\mathcal{T}^*)^+ \mapsto ((\mathcal{T}^*)^+)^* = \mathcal{T}^-$, a copy of the original $\mathcal{T}$ with an additional negative (the mirror image of a positive) ear at the branch line $[\chi(x_1)^{\infty}, \chi^2\partial^r(I)] = [(x_3)^{\infty}, \partial^r(I)]$. The subtemplate $\mathcal{T}^-$ contains the orbit $\chi(\partial_4^{\ell}(\mathcal{V}))$, which by Lemma 2 equals $\partial_2^{\ell}(\mathcal{V})$. □

The technical part of the proof of Theorem 3 is to show that we can append positive and negative ears to a copy of $\mathcal{V}_0$ in alternating fashion. To do so, we first must map $\mathcal{V}_0$ into $\mathcal{V}_0$ in such a way as to avoid either the $(x_1)^{\infty}$ or $(x_3)^{\infty}$ edge of $\mathcal{V}_0$, as required by the hypotheses of Lemmas 3 and 4. Then, after appending the appropriate ear, we send this latter $\mathcal{V}_0$ back into itself in such a way that we may iterate the procedure. This is a crucial step which depends greatly on our ability to work with subtemplates symbolically.

**Proposition 5** *The inflation $\mathfrak{H} \equiv \mathfrak{F}^*\mathfrak{D}^*\mathfrak{G}\mathfrak{F}\mathfrak{D}\mathfrak{G}^*$ takes $\mathcal{V}_0 \hookrightarrow \mathcal{V}_0$ isotopically. An intersection of the image of $\partial_2^{\ell}(\mathcal{V})$ in $\beta_1(\mathcal{V})$ is $\lhd$-minimal among all orbits in the image of $\mathfrak{H}$.*

*Proof:* The symbolic action of $\mathfrak{H}$ is

$$\mathfrak{H} \equiv \mathfrak{F}^*\mathfrak{D}^*\mathfrak{G}\mathfrak{F}\mathfrak{D}\mathfrak{G}^* : \mathcal{V}_0 \hookrightarrow \mathcal{V}_0 \qquad \begin{cases} x_1 \mapsto x_2x_3^2x_4x_1(x_2x_4)^2x_2x_3x_4x_1 \\ x_2 \mapsto x_2x_3^2x_4x_1(x_2x_4)^3x_2x_3x_4x_1 \\ x_3 \mapsto x_2x_3^2x_4x_1x_2x_4 \\ x_4 \mapsto x_2x_3^2x_4x_1x_2x_4 \end{cases} . \tag{21}$$

That this inflation is isotopic follows from repeated application of Proposition 1. It seems impossible to draw an accurate picture of the action of this inflation (the reader is encouraged to verify this). We first compute the image of the endpoints $\partial_i^{\ell/r}(\mathcal{V})$ under the inflation

$$\begin{aligned}
\mathfrak{H} &: \mathcal{V}_0 \hookrightarrow \mathcal{V}_0 \qquad (22)\\
\partial_1^{\ell}(\mathcal{V}) &\mapsto \left(x_2x_3^2x_4x_1(x_2x_4)^2x_2x_3x_4x_1\right)^{\infty}\\
\partial_1^{r}(\mathcal{V}) &\mapsto x_2x_3^2x_4x_1(x_2x_4)^2x_2x_3x_4x_1\left(x_2x_3^2x_4x_1(x_2x_4)^3x_2x_3x_4x_1x_2x_3^2x_4x_1x_2x_4\right)^{\infty}\\
\partial_2^{\ell}(\mathcal{V}) &\mapsto x_2x_3^2x_4x_1(x_2x_4)^3x_2x_3x_4x_1\left(x_2x_3^2x_4x_1x_2x_4\right)^{\infty}\\
\partial_2^{r}(\mathcal{V}) &\mapsto \left(x_2x_3^2x_4x_1(x_2x_4)^3x_2x_3x_4x_1x_2x_3^2x_4x_1x_2x_4\right)^{\infty}\\
\partial_3^{\ell}(\mathcal{V}) &\mapsto \left(x_2x_3^2x_4x_1x_2x_4\right)^{\infty}\\
\partial_3^{r}(\mathcal{V}) &\mapsto x_2x_3^2x_4x_1x_2x_4\left(x_2x_3^2x_4x_1x_2x_4x_2x_3^2x_4x_1(x_2x_4)^3x_2x_3x_4x_1\right)^{\infty}\\
\partial_4^{\ell}(\mathcal{V}) &\mapsto x_2x_3^2x_4x_1x_2x_4\left(x_2x_3^2x_4x_1(x_2x_4)^2x_2x_3x_4x_1\right)^{\infty}\\
\partial_4^{r}(\mathcal{V}) &\mapsto \left(x_2x_3^2x_4x_1x_2x_4x_2x_3^2x_4x_1(x_2x_4)^3x_2x_3x_4x_1\right)^{\infty}.
\end{aligned}$$

From (21), the image of the first $x_2$ in $\partial_2^{\ell}(\mathcal{V})$ contains two $x_1$ symbols. We claim that a shift of the image of $\partial_2^{\ell}(\mathcal{V})$ to one of these two $x_1$ symbols is $\lhd$-minimal in $\beta_1(\mathcal{V})$ among all shifts of the image of every other endpoint of $\beta(\mathcal{V})$ which begin with $x_1$. That this is so is a simple matter of choosing the shift of the image of $\partial_2^{\ell}(\mathcal{V})$ which is $\lhd$-minimal in $\beta_1(\mathcal{V})$ and then comparing this to all such shifts of the other endpoints $\mathfrak{H}(\partial_i^{\ell/r}(\mathcal{V}))$. Using the kneading ordering in (3), this can be done by hand or (more conveniently) by computer. In this manner, we calculate that

$$\sigma^{14}\mathfrak{H}(\partial_2^{\ell}(\mathcal{V})) = x_1\left(x_2x_3^2x_4x_1x_2x_4\right)^{\infty} \qquad (23)$$

is $\lhd$-minimal among all other orbits in the image of $\mathfrak{H}$ in $\beta_1(\mathcal{V})$, where $\sigma$ denotes the shift operator. $\square$

**Proposition 6** *The inflation $\mathfrak{H}^* \equiv \mathfrak{F}\mathfrak{D}\mathfrak{G}^*\mathfrak{F}^*\mathfrak{D}^*\mathfrak{G}$ takes $\mathcal{V}_0 \hookrightarrow \mathcal{V}_0$ isotopically. An intersection of the image of $\partial_4^{\ell}(\mathcal{V})$ in $\beta_3(\mathcal{V})$ is $\lhd$-minimal among all orbits in the image of $\mathfrak{H}^*$.*

*Proof:* Since $\mathfrak{H}$ is isotopic, so is the conjugate $\mathfrak{H}^*$ via Proposition 3. Apply $\chi$ to Equation (23) to show that

$$\chi\sigma^{14}\mathfrak{H}(\partial_2^{\ell}(\mathcal{V})) = \chi\left\{x_1\left(x_2x_3^2x_4x_1x_2x_4\right)^{\infty}\right\} \qquad (24)$$

is $\chi(\lhd)$-minimal in $\chi(\beta_1(\mathcal{V}))$; after an application of Lemma 2 and the fact that $\chi$ commutes with the shift operator $\sigma$,

$$\sigma^{14}\chi\mathfrak{H}(\partial_2^{\ell}(\mathcal{V})) = x_3\left(x_4x_1^2x_2x_3x_4x_2\right)^{\infty} \qquad (25)$$

is $\lhd$-minimal in $\beta_3(\mathcal{V})$. Now insert $\chi^2$ in the domain. Since $\chi$ is involutive, we have shown that

$$\sigma^{14}\chi\mathfrak{H}\chi(\chi\partial_2^\ell(\mathcal{V})) = x_3\left(x_4x_1^2x_2x_3x_4x_2\right)^\infty \tag{26}$$

or,

$$\sigma^{14}\mathfrak{H}^*(\partial_4^\ell(\mathcal{V})) = x_3\left(x_4x_1^2x_2x_3x_4x_2\right)^\infty \tag{27}$$

is $\lhd$-minimal in $\beta_3(\mathcal{V})$. $\square$

**Proposition 7** *The template $\mathcal{W}_q$ appears as a subtemplate of $\mathcal{V}_0$ for all $q > 0$.*

*Proof:* Since we will be inflating $\mathcal{V}_0 \hookrightarrow \mathcal{V}_0$ iteratively, we set some notation for distinguishing the various copies of $\mathcal{V}_0$. Let $\{\mathcal{V}^k : k = 1, 2, \ldots\}$ be a sequence of disjoint embedded templates, each of which is isotopic to $\mathcal{V}_0$. Please note the difference between superscripts and subscripts: the superscripts are used solely to label different copies of the same template.

Let $\partial_i^{\ell/r}(\mathcal{V}^1)$ for $i = 1 \ldots 4$ denote the boundary orbits of the template $\mathcal{V}^1$. These symbol sequences are the same as those in Equation (6), but we note that they refer to the edges of this *first* copy of $\mathcal{V}_0$. The symbol sequences for the boundary components $\partial_i^{\ell/r}(\mathcal{V}^k)$ for $k > 1$ are identical to those of $\mathcal{V}^1$, but they refer to orbits on *different copies* of the same template.

This is the outline of the proof: we assemble $\mathcal{W}_q$ from $\mathcal{V}^1$ by appending ears (as per Lemmas 3 and 4) along the image of $\partial_2^\ell(\mathcal{V}^1)$ in $\mathcal{V}^2$. At each stage, we embed $\mathcal{V}^k$ into $\mathcal{V}^{k+1}$ isotopically, stretching out the original $\partial_2^\ell(\mathcal{V}^1)$ to lie in the proper position to apply either Proposition 5 or 6. Two points are worthy of mention: (1) the signs of the appended ears alternates $+, -, +, -, \ldots$; and, (2) each successive ear is appended to the image of $\partial_2^\ell(\mathcal{V}^1)$ "preceding" the last appended ear (preceding in the sense of the orientation on $\partial_2^\ell(\mathcal{V}^1)$ induced by the semiflow).

Equation (28) shows the steps in building $\mathcal{W}_q$. Each arrow denotes a subtemplate inclusion. Alternating $\mathfrak{H}$ and $\mathfrak{H}^*$ sends $\mathcal{V}^k \hookrightarrow \mathcal{V}^{k+1}$ isotopically while allowing us to append positive and negative ears as in the upper sequence.

$$\begin{array}{ccccccccc} \mathcal{W}_1 & \overset{\text{append}+}{\longrightarrow} & \mathcal{W}_1^+ & \overset{\text{append}-}{\longrightarrow} & \mathcal{W}_2 & \overset{\text{append}+}{\longrightarrow} & \mathcal{W}_2^+ & \overset{\text{append}-}{\longrightarrow} & \\ & & \downarrow\subset & & \downarrow\subset & & \downarrow\subset & & \cdots \\ \mathcal{V}^1 & \xrightarrow{\mathfrak{H}} & \mathcal{V}^2 & \xrightarrow{\mathfrak{H}^*} & \mathcal{V}^3 & \xrightarrow{\mathfrak{H}} & \mathcal{V}^4 & \xrightarrow{\mathfrak{H}^*} & \end{array} \tag{28}$$

We now turn to the details of the above outline. Embed $\mathcal{V}^1$ into $\mathcal{V}^2$ via the isotopic inflation $\mathfrak{H}$. By Proposition 5, the image of $\partial_2^\ell(\mathcal{V}^1)$ is $\lhd$-minimal in $\beta_1(\mathcal{V}^2)$ among all other orbits in the image of $\mathfrak{H}$. Hence, the subtemplate $\mathfrak{H}(\mathcal{V}^1) \subset \mathcal{V}^2$ satisfies the hypotheses of Lemma 3 and we may append a positive ear along the minimal intersection of $\mathfrak{H}[\partial_2^\ell(\mathcal{V}^1)]$ in $\beta_1(\mathcal{V}^2)$. Appending a positive ear to $\mathcal{W}_1$ at that location yields a new subtemplate of $\mathcal{V}^2$ pictured in Figure 10 which we denote $\mathcal{W}_1^+$. By Lemma 3, $\mathcal{W}_1^+ \subset \mathcal{V}^2$ contains the orbit $\partial_4^\ell(\mathcal{V}^2)$.

Now map $\mathcal{V}^2$, along with its subtemplates $\mathcal{W}_1$ and $\mathcal{W}_1^+$ via the inflation $\mathfrak{H}^* : \mathcal{V}^2 \hookrightarrow \mathcal{V}^3$. By Proposition 6, this takes $\mathcal{W}_1^+$ to a "deeper" isotopic copy of $\mathcal{W}_1^+$ in $\mathcal{V}^3$ while taking

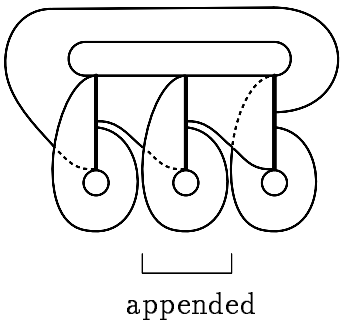


**FIGURE 10: The template $\mathcal{W}_1^+$**

$\partial_4^\ell(\mathcal{V}^2)$ to a point which is $\lhd$-minimal in $\beta_3(\mathcal{V}^3)$. The hypotheses of Lemma 4 are thus satisfied and one may append a negative ear along the intersection of $\mathfrak{H}^*[\partial_4^\ell(\mathcal{V}^2)]$ with $\beta_3(\mathcal{V}^3)$, which precedes the appended positive ear of $\mathcal{W}_1^+$ (since $\partial_4^\ell(\mathcal{V}^2)$ precedes the appended ear in $\mathcal{V}^2$); therefore, in the grand scheme, this negative ear fits "in between" the two existing positive ears. We now have an isotopic copy of $\mathcal{W}_2$ in $\mathcal{V}^3$: see Figure 11 for a schematic representation. By Proposition 6, this copy of $\mathcal{W}_2 \subset \mathcal{V}^3$ contains the orbit $\partial_2^\ell(\mathcal{V}^3)$ and this orbit precedes the appended negative ear as per Figure 11.

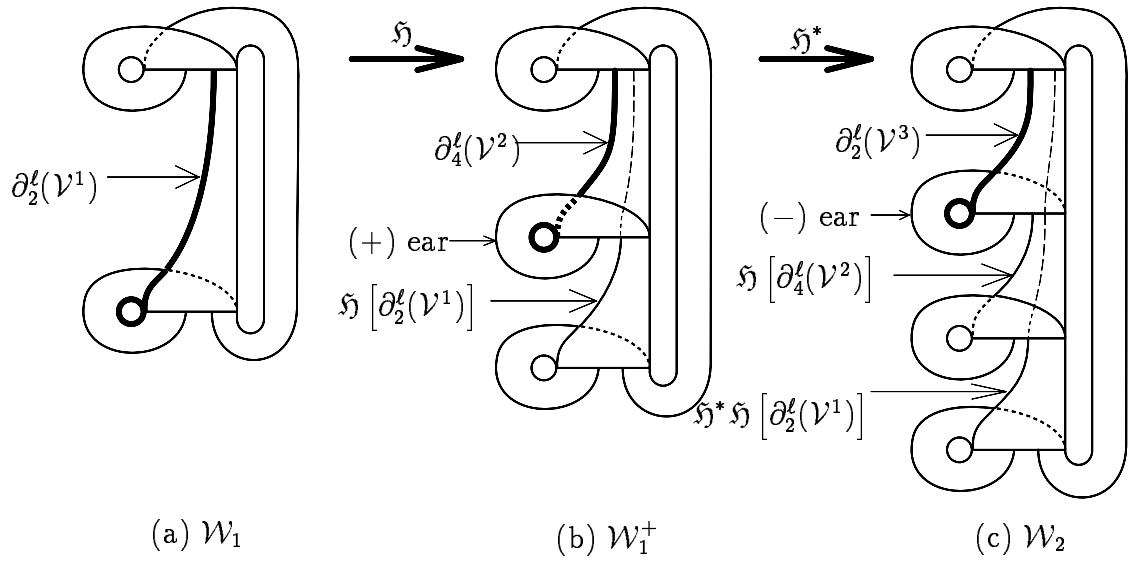


**FIGURE 11: The steps in building $\mathcal{W}_q$; (a) begin with $\mathcal{V}^1$: a copy of $\mathcal{V}_0$; (b) append a positive ear to $\mathfrak{H}[\partial_2^\ell(\mathcal{V}^1)]$ to obtain $\mathcal{W}_1^+ \subset \mathcal{V}^2$ which contains $\partial_4^\ell(\mathcal{V}^2)$ as an orbit; (c) append a negative ear to $\mathfrak{H}^*[\partial_4^\ell(\mathcal{V}^2)]$ to get $\mathcal{W}_2 \subset \mathcal{V}^3$ with $\partial_2^\ell(\mathcal{V}^3)$ as an orbit**

We now have $\mathcal{V}^3$ which contains a subtemplate $\mathcal{W}_2$ containing the orbit $\partial_2^\ell(\mathcal{V}^3)$ along which we wish to append another pair of ears. Since $\mathcal{V}^3$ is again an isotopic copy of

$\mathcal{V}^1$ with $\partial_2^\ell(\mathcal{V}^3)$ corresponding to $\partial_2^\ell(\mathcal{V}^1)$, we may now iterate the procedure. Map $\mathcal{V}^3$ into $\mathcal{V}^4$ via $\mathfrak{H}$, append a positive ear to the image of $\mathcal{W}_2$ to obtain $\mathcal{W}_2^+$, then apply $\mathfrak{H}^*$ and append a negative ear to the image of $\mathcal{W}_2^+$ to produce $\mathcal{W}_3$. Since all the inflations involved are isotopic, we continue to carry the completed $\mathcal{W}_i$ along isotopically as we append additional ears. Thus, we can embed $\mathcal{W}_q$ in $\mathcal{V}_0$ for arbitrary $q$. □

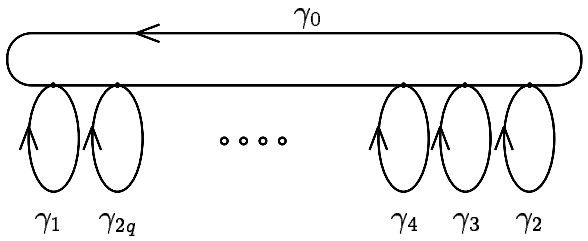


**FIGURE 12: The spine of $\mathcal{W}_q$ and the generators $\gamma_i$ of $\pi_1(\mathcal{W}_q)$**

It is difficult to keep track of the symbol sequences in order to find an explicit inflation of $\mathcal{W}_q$ into $\mathcal{V}_0$, but the essence of where $\mathcal{W}_q$ sits can be tracked easily. Crush out each strip of $\mathcal{W}_q$ in the direction transverse to the semiflow to obtain the spine and consider the generating set for $\pi_1(\mathcal{W}_q)$ given by $\{\gamma_0, \ldots, \gamma_q\}$ as in Figure 12. Then the "simplest" image of these loops in $\mathcal{V}_0$ is given by the following:

| $i$ | $\gamma_i \in \pi_1(\mathcal{W}_q)$ |
|---|---|
| 0 | $(\mathfrak{H}^*\mathfrak{H})^{q-1}(x_2x_4) = [\mathfrak{F}\mathfrak{D}\mathfrak{G}^*(\mathfrak{F}^*\mathfrak{D}^*\mathfrak{G})^2\mathfrak{F}\mathfrak{D}\mathfrak{G}^*]^{q-1}(x_2x_4)$ |
| 1 | $(\mathfrak{H}^*\mathfrak{H})^{q-1}(x_1) = [\mathfrak{F}\mathfrak{D}\mathfrak{G}^*(\mathfrak{F}^*\mathfrak{D}^*\mathfrak{G})^2\mathfrak{F}\mathfrak{D}\mathfrak{G}^*]^{q-1}(x_1)$ |
| $i = 2k > 0$ | $(\mathfrak{H}^*\mathfrak{H})^{q-k}(x_3) = [\mathfrak{F}\mathfrak{D}\mathfrak{G}^*(\mathfrak{F}^*\mathfrak{D}^*\mathfrak{G})^2\mathfrak{F}\mathfrak{D}\mathfrak{G}^*]^{q-k}(x_3)$ |
| $i = 2k+1 > 1$ | $(\mathfrak{H}^*\mathfrak{H})^{q-k-1}(x_1) = [\mathfrak{F}\mathfrak{D}\mathfrak{G}^*(\mathfrak{F}^*\mathfrak{D}^*\mathfrak{G})^2\mathfrak{F}\mathfrak{D}\mathfrak{G}^*]^{q-k-1}\,\mathfrak{F}\mathfrak{D}\mathfrak{G}^*\mathfrak{F}^*\mathfrak{D}^*\mathfrak{G}(x_1)$ |

(29)

To finish the proof of Theorem 3, we borrow some basic terminology and results from the study of braids [3, 7].

**Definition 6** *The* BRAID GROUP ON $M$ STRANDS, $B_M$, *is defined as the group generated by* $\{\sigma_i\}_1^{M-1}$ *with relations*

$$\begin{array}{ll} \sigma_i\sigma_j = \sigma_j\sigma_i & |i-j| > 1 \\ \sigma_i\sigma_j\sigma_i = \sigma_j\sigma_i\sigma_j & |i-j| = 1 \end{array} . \tag{30}$$

*Any element of $B_M$ may be geometrically realized as an embedding of the disjoint union of $M-1$ compact arcs in $\mathbb{R}^3$ with endpoints $(i,0,1)$ and $(i,0,-1)$, $i = 1, \ldots, M-1$, such that the last coordinate of each embedded arc is monotonically decreasing. In this representation, the group operation is concatenation of arcs, top to bottom, the identity element consists of the $M-1$ straight lines connecting $(i,0,1)$ to $(i,0,-1)$, and the generator $\sigma_i$ is obtained from the identity by crossing the $i$th strand over the $(i+1)$st strand with a single positive crossing.*

The relationship between braids and links crystallizes in the notion of a closed braid. Given a braid $b$, the CLOSURE, $\overline{b}$, is the link obtained by connecting the top and bottom endpoints with unknotted arcs in the simplest possible fashion: see [3, 7] for complete definitions and background.

**Lemma 5** *Let $b \in B_M$ be a braid on $M$-strands. Then $\overline{b}$, the closure of $b$, appears as a (set of) periodic orbit(s) on $\mathcal{W}_q$ for sufficiently large $q < \infty$.*

*Proof:* The concatenation of alternating positive and negative ears on $\mathcal{W}_q$ mimics the group operation of $B_M$. We first find a generating set for $B_M$ which "fits" on a finite concatenation of alternating ears, as occurs in $\mathcal{W}_q$. Figure 13 shows how to put the word $\sigma_1\sigma_2\ldots\sigma_k$ on a positive ear and $\sigma_1^{-1}\sigma_2^{-1}\ldots\sigma_k^{-1}$ on a negative ear. In particular, we can explicitly get $\sigma_1$ and $\sigma_1^{-1}$ on a single positive (negative resp.) ear. Assuming that we can find the generators $\sigma_1, \sigma_1^{-1}, \sigma_2, \sigma_2^{-1}, \ldots, \sigma_k, \sigma_k^{-1}$ on a finite sequence of ears, we can construct $\sigma_{k+1}$ and $\sigma_{k+1}^{-1}$ by concatenating additional ears as follows:

$$\begin{aligned} \sigma_{k+1} &= (\sigma_k^{-1})\ldots(\sigma_2^{-1})(\sigma_1^{-1})(\sigma_1\sigma_2\ldots\sigma_{k+1}) \\ \sigma_{k+1}^{-1} &= (\sigma_k)\ldots(\sigma_2)(\sigma_1)(\sigma_1^{-1}\sigma_2^{-1}\ldots\sigma_{k+1}^{-1}). \end{aligned} \tag{31}$$

By induction, each generator for $B_M$ fits on a finite sequence of positive and negative ears and $b$ can be built from a finite sequence of these generators.

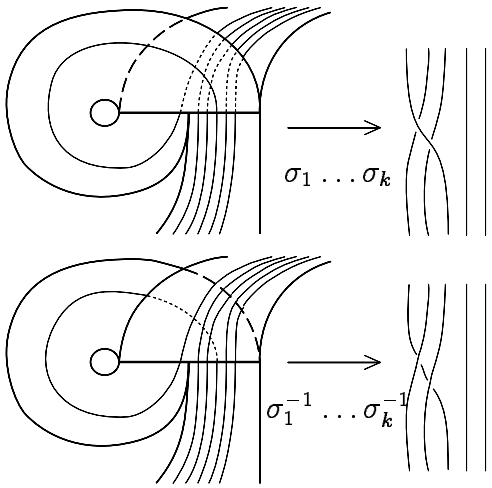


**FIGURE 13: Fitting a generating set for $B_M$ on the ears of $\mathcal{W}_q$**

There is an obstacle to fitting the closure $\overline{b}$ on the *expanding* semiflow of $W_q$ if any component has a repeating symbol sequence. To prevent this, note that since only one strand of $\overline{b}$ goes around each ear of $\mathcal{W}_q$, $\overline{b}$ does not contain two components with the same itinerary as long as each strand loops around at least one of the ears of $\mathcal{W}_q$. From (31), this will necessarily occur if $b \in B_M$ contains either $\sigma_{M-1}$ or $\sigma_{M-1}^{-1}$. If such is not the case, then we modify $b$ to $b'$,

$$b' = \left[\sigma_{M-1}\sigma_{M-1}^{-1}\right] b. \tag{32}$$

This new braid is equivalent to $b$ in $B_M$ (hence, the closures are isotopic), but this now appears as a periodic orbit set on the expanding semiflow of $\mathcal{W}_q$ (for some $q$) with certainty. □

*Proof of Theorem 3*: by Lemma 5, we can find any closed braid $\overline{b}$ as a periodic orbit set on some $\mathcal{W}_q$. By Proposition 7, every $\mathcal{W}_q \subset \mathcal{V}_0$; hence, we have shown that $\mathcal{V}_0$ contains all closed braids. By a theorem of Alexander (see [1, 3, 7]), $\mathcal{V}_0$ contains all knots and links. □

**Remark 3** The algorithm detailed here is not intended to supply the "simplest" version of a closed braid in $\mathcal{V}_0$. Consider Conjecture 1 concerning the existence of a figure-eight knot ($K_8$) in a flow. A careful attempt to draw $K_8$ on $\mathcal{V}_0$ will frustrate the reader. We can write the closed braid form of this knot as follows:

$$K_8 = \overline{\left(\sigma_2\sigma_1^{-1}\right)^2} = \overline{()(\sigma_1^{-1})(\sigma_1\sigma_2)(\sigma_1^{-1})()(\sigma_1^{-1})(\sigma_1\sigma_2)(\sigma_1^{-1})}. \tag{33}$$

One may thus fit the figure eight knot on $\mathcal{W}_4 \subset \mathcal{V}_0$. By using the table in (29), we calculate this representation of the figure-eight knot in $\mathcal{V}_0$ (the simplest known example) to cross the branch lines $11,358,338$ times (i.e., this is the minimal period of the itinerary). The symbolic methods used in this proof evidently extract some very deep information.

Theorem 3 has a number of interesting consequences related to UNIVERSAL TEMPLATES; that is, embedded templates which support all links.

**Corollary 2** *Each of the embedded templates $\{\mathcal{U}_n, \mathcal{V}_n\}$ for $n \in \mathbb{Z}$ is universal, as is any template that contains any of these as subtemplates.*

*Proof:* Theorem 2. □

**Corollary 3** *All the Lorenz-like templates $\mathcal{L}(0,n)$ for $n < 0$ are universal, hence equivalent.*

*Proof:* A Lorenz-like template is a generalization of the Lorenz template studied in [4, 36, 37] (see Figure 2(b)). Figure 14 illustrates this family: there is a single branch line with $n$ signed half-twists in the $x_2$-strip. In [31], it was shown that $\mathcal{L}(0,n) \subset \mathcal{L}(0,n-2)$ for all $n$, and that $\mathcal{L}(0,-4) \subset \mathcal{L}(0,-1)$. In [33], M. Sullivan showed that $\mathcal{U}_0 \subset \mathcal{L}(0,-2)$. □

We note that all of these relations [and others] among Lorenz-like templates have nice interpretations as template inflations. For example, it is an exercise for the curious reader to show that

$$\begin{aligned} x_1 &\mapsto x_1 \\ x_2 &\mapsto x_1 x_2^2 \end{aligned} \tag{34}$$

is an isotopic inflation of $\mathcal{L}(0,-2) \hookrightarrow \mathcal{L}(0,-1)$. It is interesting to note that while $\mathcal{L}(0,-1)$ is a universal template, $\mathcal{L}(0,1)$ does not even support all torus knots [23]. In [17], we showed that for $mn \geq 0$, $\mathcal{L}(m,n)$ is universal if and only if $m = 0$ and $n < 0$ or *vice versa*.

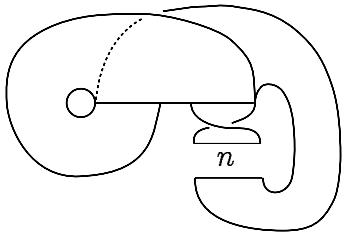


**FIGURE 14: The Lorenz-like templates $\mathcal{L}(0,n)$**

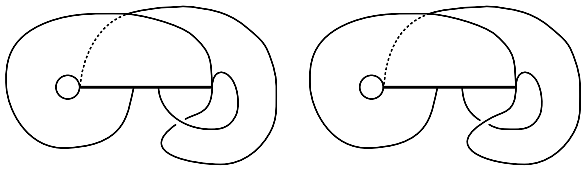

**FIGURE 15: $\mathcal{L}(0,1)$ (left) does not contain all torus knots, while $\mathcal{L}(0,-1)$ (right) is universal**

The richness of these universal templates goes far beyond that expressed in the original conjecture of [5]: besides containing all knots, this class of universal templates contains all links. By Proposition 4, we can also find a countable infinity of disjoint, separable copies of $\mathcal{V}_0$ isotopically embedded in $\mathcal{V}_0$, each of these containing all closed braids. The properties of these ostensibly simple templates are pleasantly surprising.

It follows from Corollaries 2 and 3 that most every template thus far appearing in the literature which has a combination of positive and negative crossings is in fact universal. This sheds light on the difficulty of finding invariants for such templates. Invariants for positive templates (where the crossings are all of one sign and which hence cannot be universal) have been found [32], but as yet, none exist for mixed-crossing templates. It is now clear that any such invariant which measures only the spectrum of different orbit embeddings would be very inefficient at distinguishing mixed templates, since many such templates are universal. The question of template equivalence should therefore be refined to a more restrictive notion.

Perhaps a good approach would be to study the subtemplate structure of a universal template. Several open question present themselves. If a template $\mathcal{T}$ contains, e.g., $\mathcal{V}_0$ as a subtemplate, must it be the case that $\mathcal{T} \subset \mathcal{V}_0$ as well? If a template $\mathcal{T}$ contains all links, must it follow that $\mathcal{V}_0 \subset \mathcal{T}$? Were this the case, the term "universal" would be well-deserved; if not, then there may be invariants which distinguish universal templates.

# 4 FIBRATIONS OF KNOT COMPLEMENTS

Besides applications to template theory, Theorem 3 has implications for flows induced by fibrations of knots and links whose monodromies are of pseudo-Anosov type (in the Thurston classification [34, 9]).

**Definition 7** *A knot or link $K$ in $S^3$ is* FIBRED *if there is a fibration $p : S^3 \setminus K \to S^1$ with fibre a Seifert spanning surface $M^2$ [28, 7]. The fibration induces a diffeomorphism $\Phi$ on the fibre called the* MONODROMY *of the fibration. The* INDUCED FLOW *for the fibration is that obtained by integrating $\nabla p$, the gradient, or, equivalently, by embedding the suspension flow of the monodromy $\Phi$.*

By invoking the Thurston classification of surface diffeomorphisms [34, 9], we can speak of "the" fibration for $K$. For example, the figure-eight knot is fibred with fibre a punctured torus and monodromy isotopic to the Anosov map,

$$\Phi = \begin{bmatrix} 2 & 1 \\ 1 & 1 \end{bmatrix}, \tag{35}$$

acting on the universal cover $\mathbb{R}^2 \setminus \mathbb{Z}^2$. The closed orbits of the induced flow (the suspension of $\Phi$) are the subject of [5] and of Conjecture 1, which we now resolve.

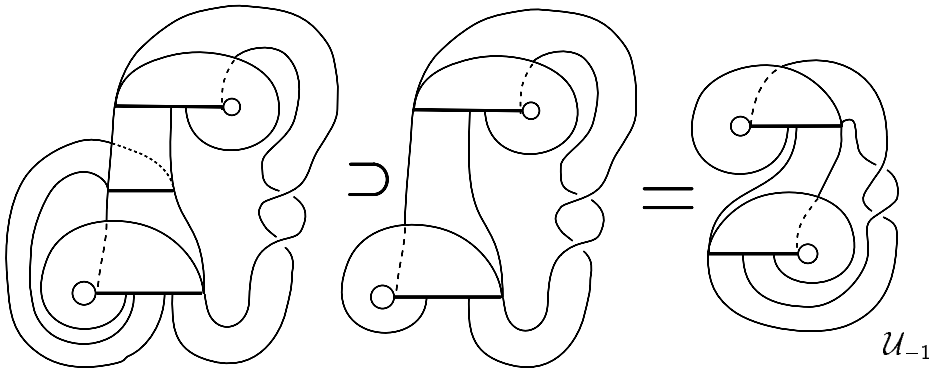


**FIGURE 16: $\mathcal{U}_{-1}$ (right) as a subtemplate of the direct version of the figure-eight template (left).**

**Theorem 4** *Any flow transverse to a fibration over $S^1$ of the figure-eight knot complement in $S^3$ contains every knot and link as closed orbits.*

*Proof:* In [5] Birman and Williams derive two templates for the flow induced by integrating the gradient of the fibration of the figure-eight knot complement (corresponding to the unique pseudo-Anosov monodromy $\Phi$) — one by means of direct visualization, and the other indirectly by means of branched coverings of $S^3$. The direct version appears

in the left in Figure 16 and the indirect version in Figure 17. It was noted in [5] that a direct proof of the equivalence of these two templates seemed highly nontrivial. In Figure 16, we show that the "direct" version contains $\mathcal{U}_{-1}$ as a subtemplate. This is accomplished by ignoring one strip and noting that all remaining orbits must live on the original template. By Corollary 2, this version of the figure-eight template is universal. In [33], it was shown that the "indirect" version contains $\mathcal{V}_0$ as a subtemplate (we give an alternate proof in Proposition 8 below) and hence is also universal.

These templates correspond to the particular flow induced by the fibration which has pseudo-Anosov monodromy; however, pseudo-Anosov maps minimize dynamics, so any other fibration in the isotopy class has at least the periodic orbits that the pseudo-Anosov case has [2]. Any flow which is transverse to such a fibration is isotopic to one which is obtained by integrating the gradient. □

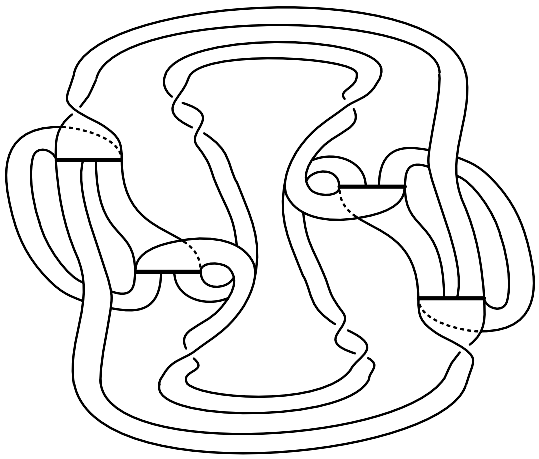

**FIGURE 17: The "indirect" branched-covering version of the figure-eight template**

The following is a worthwhile (though potentially difficult) question to pursue:

**Question 1** *Which fibred knots possess all knots and links as closed orbits of the fibration-induced flow on their complements?*

Question 1 is relevant for knowing which fibred knots or links do *not* support every link as closed orbits of the fibration-induced flow, since, for fibred knots or links, the link of closed orbits of this flow forms an invariant for the knot [5]. We can at this time provide only a partial answer to this question:

**Proposition 8** *The closure of any braid of the form* $\left(\sigma_1\sigma_2^{-1}\right)^k$ *for* $|k| > 1$ *is a fibred link with fibration supporting all knots and links as closed orbits. In particular, the Borromean rings* ($k = 3$) *shares this property.*

*Proof:* Assume $k > 1$. After Birman and Williams, we examine $k$-fold branched covers of $S^3$ branched over the unknotted closed braid $b = \overline{\sigma_1\sigma_2^{-1}}$. They show in [5] that the

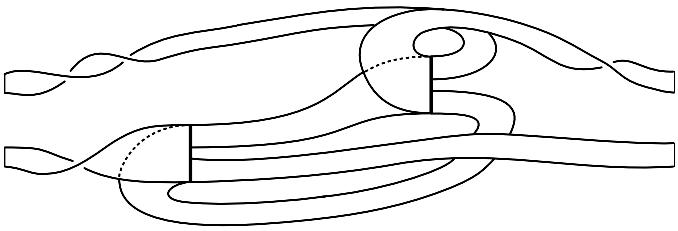

**FIGURE 18: The fundamental template component of the branched $k$-fold cyclic cover of $S^3$.**

template for the fibration of the complement of $b$ consists of $k$-copies of the template pictured in Figure 18 glued together end-to-end in cyclic fashion. In particular, note that the indirect model of the figure-eight template in Figure 17 corresponds to the case $k = 2$. Take two copies of the template of Figure 18 glued at one end as in Figure 19(a). This object appears naturally within the template for the complement of the closed braid for $k > 1$. In Figure 19(b)-(e) we ignore the loose ends of this object and isotope it to reveal a copy of $\mathcal{V}_0$ which therefore sits in the template for the complement of the closed braid when $k > 1$. For $k < -1$, note that the braid (hence the template) is the mirror image of that for $k > 1$. The mirror image of a universal template is again universal. □

Proposition 8 specifies an infinite collection of fibred knots and links with fibration-induced flows supporting all knots and links as closed orbits. We have also shown [15] that the Whitehead link shares this property. The class of fibred links whose induced flows contain all links as closed orbits must be from the class which have pseudo-Anosov type monodromy, and which are not positive braids. Question 1 is related to the more fundamental question:

**Question 2** *What are necessary and sufficient conditions for a template $\mathcal{T} \subset S^3$ to be universal?*

Even a basic set of sufficient conditions could provide some nice forcing theorems. Of course, one necessary condition is that the template contain crossings of both positive and negative type. This is not sufficient, however, as one may for example embed $\mathcal{V}_0$ in $S^3$ so that the $x_4$ strip is tied in a nontrivial knot $K$. Then all knots on this new template would be satellites of the knot $K$: such satellites will always be "more complicated" than $K$ [7], so this template cannot be universal. It is difficult to formulate a simple conjecture to Question 2.

# 5 CONCLUSIONS

Our results on the existence of templates which support all tame links as periodic orbits open up some new directions (and close others) in the study of templates. The original motivation for studying template knots for fibred links in [5] rested on the fact that the

link of periodic orbits on the template is an invariant of the knot. We now see that this invaraint is weak in a number of cases. While it is now less clear what it means for two templates to be "equivalent," we do have new techniques for their analysis which do not rely entirely upon direct pictorial constructions.

The existence of universal templates provides a wealth of examples of interesting three-dimensional flows, along with some counterintuitive facts about the set of all links. On the one hand, it is possible to fit (up to isotopy) every possible embedding of a disjoint set of 1-spheres on a simple embedded branched 2-manifold. And within these, Proposition 4 implies a self-similarity among this set. On the other hand, since a pseudo-Anosov map of a surface has a dense periodic set [9], the fibration of the complement of the figure-eight knot induces a flow on $S^3$ whose periodic orbit set is dense in $S^3$ and exhausts all knot and link isotopy classes. The fact that we can fill up $S^3$ or $\mathcal{V}_0$ densely with the same set of links is a beautiful feature of templates.

One may regard a universal template as a "closure" of the space of all knots or links, which immediately calls to mind Thurston's theory of the space of embedded curves on a surface [34, 9]. The closures induced by the universal templates we have described do not appear to share the beautiful properties that Thurston's closures do, however. The self-similarity implied by Proposition 4 (and, in general, by the limits of iterated isotopic renormalizations) suggests that a template gives a very convoluted sort of completion: e.g., numerical invariants of the knots on a template do not extend naturally to a continuous function on non-periodic orbits.

There are other implications which we do not describe in this paper, mostly in connection with ODEs and global bifurcations of periodic orbits in parametrized flows. Notable among them is the following, explored in detail in [14]:

**Theorem 5** *There exists an open set of parameters $\beta \in [6.5, 10.5]$ for which periodic solutions to the differential equation*

$$\begin{aligned} \dot{x} &= 7[y - \phi(x)], \\ \dot{y} &= x - y + z, \\ \dot{z} &= -\beta y, \\ \phi(x) &= \frac{2}{7}x - \frac{3}{14}\left[|x+1| - |x-1|\right], \end{aligned} \tag{36}$$

*contain representatives from every knot and link equivalence class.*

Equation (36) is a PL-vector field modeling an electric circuit [8].

# ACKNOWLEDGEMENTS

The author would like to acknowledge the enthusiastic support and remarks of Philip Holmes. Conversations with Mike Sullivan, Allen Hatcher, Keith Burns, Dennis Sullivan, John Smillie, John Franks, Phil Boyland, Krystyna Kuperberg, and Marcy Barge were also beneficial. This work was completed with the support of the National Science Foundation and the hospitality of the Program in Applied and Computational Mathematics, Princeton University.

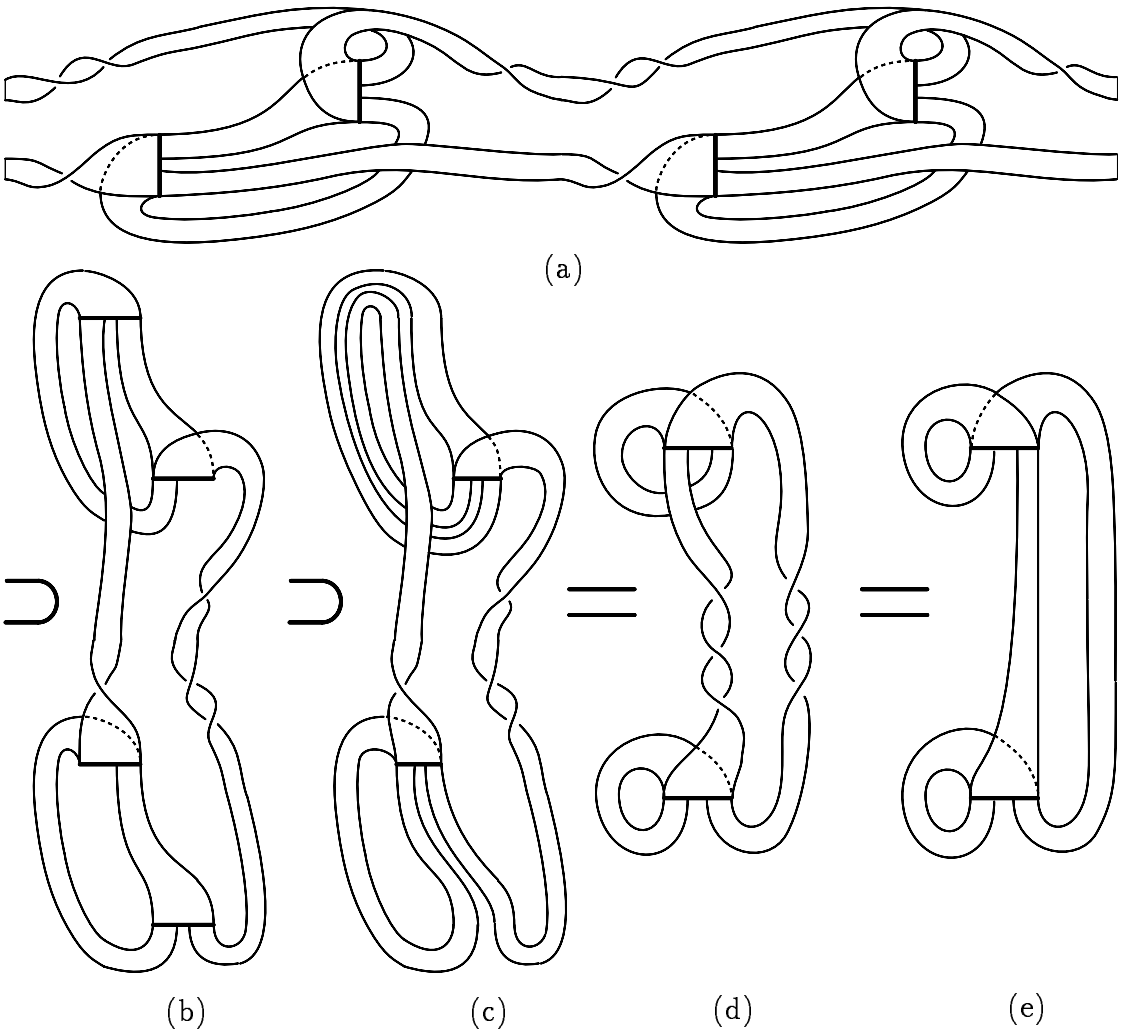


**FIGURE 19:** (a) the 2-fold copy of the fundamental template component; (b) ignore the loose ends (and rotate); (c) remove the extraneous branch lines; (d) pull out a full positive twist; (e) the twists cancel to reveal $\mathcal{V}_0$

# REFERENCES


[1] J. W. Alexander. A lemma on systems of knotted curves. *Proc. Nat. Acad. Sci. USA*, 9:93–95, 1923.

[2] D. Asimov and J. Franks. Unremovable closed orbits. In J. Palis, editor, *Geometric Dynamics, Lecture Notes in Mathematics 1007*. Springer-Verlag, 1983.

[3] J. Birman. *Braids, Links, and Mapping Class Groups*. Princeton University Press, Princeton, N.J., 1974.

[4] J. Birman and R. F. Williams. Knotted periodic orbits in dynamical systems–I : Lorenz's equations. *Topology*, 22(1):47–82, 1983.

[5] J. Birman and R. F. Williams. Knotted periodic orbits in dynamical systems–II : knot holders for fibered knots. *Cont. Math.*, 20:1–60, 1983.

[6] R. Bowen. On Axiom A diffeomorphisms. In *Regional Conference Series in Mathematics 35*, pages 1–45. National Science Foundation, American Mathematical Society, 1978.

[7] G. Burde and H. Zieschang. *Knots*. De Gruyter, Berlin, 1985.

[8] L. Chua, M. Komuro, and T. Matsumoto. The double scroll family. *IEEE Trans. on Circuits and Systems*, 33:1073–1118, 1986.

[9] A. Fathi, F. Laudenbach, and V. Poenaru et al. Travaux de Thurston sur les surfaces. *Astérique*, 66-67:1–284, 1979.

[10] J. Franks. Knots, links, and symbolic dynamics. *Ann. of Math.*, 113:529–552, 1981.

[11] J. Franks and R. F. Williams. Entropy and knots. *Trans. Am. Math. Soc.*, 291(1):241–253, 1985.

[12] J. Franks and R. F. Williams. Braids and the Jones polynomial. *Trans. Am. Math. Soc.*, 303(1):97–108, 1987.

[13] R. Ghrist and P. Holmes. Knots and orbit genealogies in three dimensional flows. In *Bifurcations and Periodic Orbits of Vector Fields*, pages 185–239. NATO ASI series C volume 408, Kluwer Academic Press, 1993.

[14] R. Ghrist and P. Holmes. An ODE whose solutions contain all knots and links. To appear in *Intl. J. Bifurcation and Chaos*, 1996.

[15] R. Ghrist, P. Holmes, and M. Sullivan. Knots and links in three-dimensional flows. In preparation, December 1995.

[16] R. W. Ghrist. Flows on $S^3$ supporting all links as closed orbits. *Electronic Research Announcements AMS*, 1 (2):91–97, 1995.

[17] R. W. Ghrist. *The Link of Periodic Orbits for a Flow*. PhD thesis, Cornell University, 1995.

[18] J. Guckenheimer and P. J. Holmes. *Nonlinear Oscillations, Dynamical Systems, and Bifurcations of Vector Fields*. Springer-Verlag, New York, 1983.

[19] P. J. Holmes. Bifurcation sequences in the horseshoe map: infinitely many routes to chaos. *Phys. Lett. A*, 104:299–302, 1984.

[20] P. J. Holmes. Knotted periodic orbits in suspensions of Smale's horseshoe: period mutiplying and cabled knots. *Physica D*, 21:7–41, 1986.

[21] P. J. Holmes. Knotted periodic orbits in suspensions of annulus maps. *Proc. Roy. London Soc. A*, 411:351–378, 1987.

[22] P. J. Holmes. Knotted periodic orbits in suspensions of Smale's horseshoe: extended families and bifurcation sequences. *Physica D*, 40:42–64, 1989.

[23] P. J. Holmes and R. F. Williams. Knotted periodic orbits in suspensions of Smale's horseshoe: torus knots and bifurcation sequences. *Archive for Rational Mech. and Anal.*, 90(2):115 –193, 1985.

[24] Lj. Kocarev, D. Dimovski, Z. Tasev, and L. Chua. Topological description of a chaotic attractor with spiral structure. *Phys. Lett. A*, 190:399–402, 1994.

[25] J. Milnor and W. Thurston. On iterated maps of the interval I and II. Unpublished notes, Princeton University, 1977.

[26] G. B. Mindlin, H. S. Solari, M. A. Natiello, R. Gilmore, and X. J. Hou. Topological analysis of chaotic time series data from the Belousov-Zhabotinskii reaction. *J. Nonlinear Sci.*, 1:147–173, 1991.

[27] C. Robinson. *Dynamical Systems: Stability, Symbolic Dynamics, and Chaos*. CRC Press, Ann Arbor, MI, 1995.

[28] D. Rolfsen. *Knots and Links*. Publish or Perish, Berkely, CA, 1977.

[29] S. Smale. Differentiable dynamical systems. *Bull. Am. Math. Soc.*, 73:747–817, 1967.

[30] M. C. Sullivan. Composite knots in the figure-8 knot complement can have any number of prime factors. Preprint, June 1992.

[31] M. C. Sullivan. Prime decomposition of knots in Lorenz-like templates. *J. Knot Thy. and Ram.*, 2(4):453–462, 1993.

[32] M. C. Sullivan. A zeta function for positive templates and a general template invariant. Preprint, April 1993.

[33] M. C. Sullivan. The prime decomposition of knotted periodic orbits in dynamical systems. *J. Knot Thy. and Ram.*, 3(1):83–120, 1994.

[34] W. P. Thurston. On the geometry and dynamics of diffeomorphisms of surfaces. *Bull. Am. Math. Soc.*, 19(2):417–431, 1988.

[35] N. B. Tufillaro, H. Solari, and R. Gilmore. Relative rotation rates: fingerprints for strange attractors. *Phys. Rev. A*, 41(10):5717–5720, 1990.

[36] R. F. Williams. The structure of Lorenz attractors. In S. Smale A. Chorin, J. E. Marsden, editor, *Turbulence Seminar, Berkeley 1976/77*, pages 94–116. Springer Lecture Notes in Math. Vol. 615, 1977.

[37] R. F. Williams. The structure of Lorenz attractors. *Inst. Hautes Études Sci. Publ. Math.*, 50:73–79, 1979.

[38] R. F. Williams. Lorenz knots are prime. *Ergod. Th. and Dynam. Sys.*, 4:147–163, 1983.

# List of Figures